


The miR164-GhCUC2-GhBRC1 module regulates plant architecture through abscisic acid in cotton

Jingjing Zhan¹, Yu Chu¹, Ye Wang¹, Yangyang Diao¹, Yanyan Zhao¹, Lisen Liu¹, Xi Wei¹, Yuan Meng¹, Fuguang Li^{1,2,*} and Xiaoyang Ge^{1,2,*} 

¹State Key Laboratory of Cotton Biology, Institute of Cotton Research of Chinese Academy of Agricultural Sciences, Anyang, China

²Zhengzhou Research Base, State Key Laboratory of Cotton Biology, Zhengzhou University, Zhengzhou, China

Received 12 November 2020;

revised 11 March 2021;

accepted 28 March 2021.

*Correspondence (Tel +86 03722562204;

fax +86 03722562256; email

gexiaoyang@caas.cn (X.G.)

(Tel +86 03722562204; Fax +86

03722562256; email aylifug@caas.cn (FL))

Summary

Branching determines cotton architecture and production, but the underlying regulatory mechanisms remain unclear. Here, we report that the *miR164-GhCUC2* (CUP-SHAPED COTYLEDON2) module regulates lateral shoot development in cotton and *Arabidopsis*. We generated OE-GhCUC2m (overexpression *GhCUC2m*) and STTM164 (short tandem target mimic RNA of *miR164*) lines in cotton and heterologous expression lines for *gh-miR164*, *GhCUC2* and *GhCUC2m* in *Arabidopsis* to study the mechanisms controlling lateral branching. *GhCUC2m* overexpression resulted in a short-branch phenotype similar to STTM164. In addition, heterologous expression of *GhCUC2m* led to decreased number and length of branches compared with wild type, opposite to the effects of the OE-gh-pre164 line in *Arabidopsis*. *GhCUC2* interacted with *GhBRC1* and exhibited similar negative regulation of branching. Overexpression of *GhBRC1* in the *brc1-2* mutant partially rescued the mutant phenotype and decreased branch number. *GhBRC1* directly bound to the *NCED1* promoter and activated its transcription, leading to local abscisic acid (ABA) accumulation and response. Mutation of the *NCED1* promoter disrupted activation by *GhBRC1*. This finding demonstrates a direct relationship between *BRC1* and ABA signalling and places ABA downstream of *BRC1* in the control of branching development. The *miR164-GhCUC2-GhBRC1-GhNCED1* module provides a clear regulatory axis for ABA signalling to control plant architecture.

Keywords: *miR164*, *GhCUC2*, *GhBRC1*, ABA, lateral branch.

Introduction

Plant architecture, the physiological pattern of flower and lateral organ development, is a major determinant of planting area, cultivation pattern, grain productivity and planting efficiency in crops (Wang and Li, 2008). Xinjiang is currently the largest and highest-yielding cotton growing area in China, and compact plant architecture is required for cotton cultivars grown in this region to increase planting density and facilitate mechanical harvesting. Branches contribute to bud initiation, activation and expansion and sustained lateral growth. This process is regulated by a complex network of phytohormones and regulatory factors and ultimately governs aerial plant architecture and plant yield (Wang *et al.*, 2018).

In recent years, some studies have identified the transcription factors that participate in initiation of axillary meristems, and subsequently, the formation of plant branches. The TCP transcription factor TEOSINTE BRANCHED1 (TB1) was found to participate in repressing bud development, resulting in decreased branching (Poza-Carrión *et al.*, 2007). Transgenic rice plants overexpressing *OsTB1* exhibited markedly reduced lateral branching, while an *OsTB1* loss-of-function mutant, *fine culm1* (*fc1*), had enhanced lateral branching (Takeda *et al.*, 2010). The tomato *BLIND* gene, encoding an MYB transcription factor, was reported to control the formation of lateral meristems (Schmitz *et al.*, 2002). GRAS transcription factors, including LATERAL

SUPPRESSOR (*LAS*) in *Arabidopsis*, lateral suppressor (*LS*) of tomato (*Solanum lycopersicum*) and MONOCULM1 (*MOC1*) in rice (*Oryza sativa*), were all found to regulate axillary meristem initiation (Greb *et al.*, 2003). The *Arabidopsis las* mutant lost the ability to form lateral shoots during vegetative development. In rice, the *moc1* mutant failed to develop tillers due to defects in axillary meristem formation, which is similar to the *ls* mutant tomato phenotype (Li *et al.*, 2003; Schumacher *et al.*, 1999). TIE1 promoted cotton branching via repressing the transcription activity of TCPs (Diao *et al.*, 2019). Mutation of SP homologs promoted short-branching architecture in cotton, and dynamic changes in *GhSFT* and *GhSP* expression level regulated cotton monopodial and sympodial branching architecture (McGarry *et al.*, 2016; Si *et al.*, 2018). While these studies have provided major in-roads for understanding the regulation of branch development, a cohesive picture of the molecular mechanisms controlling shoot branching architecture is still unavailable.

NAC (e.g. NAM, ATAF1, ATAF2 and CUC2) proteins comprise one of the largest families of plant-specific transcription factors, which is present in a wide range of land plants and has more than 100 members identified in *Arabidopsis* (Olsen *et al.*, 2005). Unsurprisingly, only a portion of NAC proteins has been studied to date, although genes in this family have been implicated in a diverse range of processes, including formation of secondary wall, controlling flowering time, age-dependent senescence, seed germination and floral and vegetative development (Mathew

and Agarwal, 2018; Mitsuda *et al.*, 2005; Saad *et al.*, 2013). Also, NAC proteins are important in the formation and maintenance of different meristem tissues and shoot branching development. NAC genes *CUC2/CUC3* directly bind to the promoter of *DA1* and activate its expression to control axillary meristem initiation and branching development (Li *et al.*, 2020). *CUC1* protein activates expression of *LSH4* and its homolog *LSH3* in shoot organ boundary cells and suppresses organ differentiation in the boundary region (Takeda *et al.*, 2011). Overexpression of *OsNAC2* contributes to tiller bud outgrowth and regulates shoot branching in rice (Mao *et al.*, 2007). The expression patterns and mutant phenotypes of *NAM*, *CUC1* and *CUC2* suggest that their function is both similar and conserved in boundary specification and shoot apical meristem (SAM) formation (Chang *et al.*, 2020; Cui *et al.*, 2016; Raman *et al.*, 2010; Vroemen *et al.*, 2003; Wang *et al.*, 2020).

NAC genes participate in auxin and abscisic acid (ABA) signal transduction and regulation of senescence (Guo and Gan, 2010), and ABA negatively regulates axillary bud growth in plants (Yao and Finlayson, 2015). Enhanced *NCED3* expression led to ABA accumulation, thus suppressing bud and branching development. Reduced ABA level in buds increased branching in *hb21*, *hb40* and *hb53* triple mutants (González-Grandío *et al.*, 2017). The complex regulation of NAC transcription factors includes microRNA (miRNA)-mediated cleavage of mRNAs (Wang *et al.*, 2020). In *Arabidopsis thaliana*, the CUP-SHAPED COTYLEDON (*CUC*) genes *CUC1* and *CUC2*, which are negatively regulated by miR164, were shown to be involved in SAM and boundary formation (Aida and Tasaka, 2006). In particular, zma-miR164e was demonstrated to cleave the mRNAs of *Arabidopsis CUC1*, *CUC2* and *NAC6* *in vitro*. Overexpression of zma-miR164e resulted in failure to form seeds and increased branch number in *Arabidopsis* via down-regulation of these genes (Liu *et al.*, 2020). Although *CUC2* participates in controlling the initiation of axillary meristems, no NAC genes have been identified to regulate cotton branching, and the direct molecular link between *CUC2* and other architecture regulation genes including *TCPs*, *NCEDs*, etc. remains unknown.

Here, we show that *GhCUC2* is cleaved by gh-miR164, and that *GhCUC2* with mutated target sequence could not be cleaved by miR164. *GhCUC2* physically interacts with a previously known lateral branch development-related protein GhBRC1 and activates its transcriptional activity to regulate lateral branch development (Diao *et al.*, 2019). In addition, genetic analysis demonstrated that *GhCUC2* and *GhBRC1* negatively regulate branching, exerting the opposite effect of miR164. This study provides novel insights into the regulatory network of *CUC2* genes lateral branch development in which a miR164-GhCUC2-GhBRC1-GhNCED1 regulatory module controls aerial plant architecture in cotton.

Results

RNA-seq and cluster analysis show differential *GhCUC2* up-regulation in short-branch cotton

To mine the differentially expressed genes (DEGs) controlling branch length in cotton, we used RNA-Seq to investigate differences in the expression profiles within axillary buds (see Figure S1 for sampling position) among three short-branch cultivars (Shan 4080, Jin7, Changrongzhongmian) and three long-branch cultivars (Zhong24, Zhong6, TM-1) of upland cotton, *Gossypium hirsutum*. Correlation and clustering analysis among the six inbred cultivars revealed that the three short-branch and

three long-branch materials, respectively, clustered together supporting that a set of specific DEGs participate in regulating cotton architecture differently between the two cultivar types (Figure 1a). To uncover the genetic underpinnings of branch length, we then identified the DEGs between the two architecture types (Figure 1b) and selected the DEGs with similar expression trends in the three short-branch materials but opposite expression trends in the long-branch materials for further analysis. This set was largely comprised of putative NAC family transcription factors, TCP family transcription factors and some HB family transcription factors (Table S1).

A recent report indicated that the *CUC2/CUC3-DA1-UBP15* regulatory module controls the initiation of axillary meristems, determining the number of lateral branches in *Arabidopsis thaliana* (Li *et al.*, 2020). In addition, *OsNAC2* has been reported to be involved in lateral shoot branching (Mao *et al.*, 2007). In the light of the conserved function of *CUC2* in shoot branching, we conducted a phylogenetic analysis of *GhCUC2*, *AtCUC2*, *OsNAC2* and several other homologous genes, which showed that *GhCUC2* is the closest homolog of *AtCUC2*, *OsNAC2* and *Petunia NAM* (Figure 1c). Furthermore, the expression levels of *GhCUC2* were significantly higher in short-branch cultivars than in long-branch cultivars, supporting a close correlation between *GhCUC2* expression and cotton branch length (Figure 1d,e). We then carried out fluorescence *in situ* hybridization (FISH) assays to determine the tissue-specific expression patterns of *GhCUC2*, which revealed that it was preferentially expressed in the axillary bud (Figure 1f). These results showing preferential expression in axillary buds and differential up-regulation in short-branch materials together support that *GhCUC2* may regulate the formation of lateral branches.

CUC2 mRNA cleavage is directed by miR164

To date, the majority of previously identified target genes of miR164-mediated regulation belong to the NAC gene family, including At-miR164-AtCUC1/CUC2/CUC3 in *Arabidopsis* (Lee *et al.*, 2017), Ade-miR164-AdNAC6/7 in *Actinidia* spp. (Wang *et al.*, 2020) and the NAC family genes *OMTN1-OMTN6* in rice (Yu *et al.*, 2014). However, miR164 targets in cotton have yet to be identified. To this end, we used degradome sequencing to accurately predict miR164 target genes and cleavage sites. Degradome sequencing indicated a significant cleavage site located at nt position 517 in *GhCUC2*, and the predicted miRNA-mediated cleavage site matched the peak (Figure 2a). High base pairing between miR164 and the *CUC2* genes suggested that miR164 can potentially establish regulatory module(s) with *CUC2*.

To obtain direct evidence that miR164 can mediate the cleavage of *CUC2* mRNA, we constructed three vectors as follows: 35s::*gh-pre164*, 35s::*GhCUC2::eGFP* and 35s::*GhCUC2m::eGFP*. *CUC2m* was designed by introducing four synonymous nucleotides into the miR164 complementary region of *CUC2* mRNA sequence (Figure 2b). *Agrobacterium tumefaciens* harbouring plasmid 35S::*gh-pre164* and 35S::*GhCUC2::eGFP* were co-transformed into tobacco (*Nicotiana benthamiana*) leaves by infiltration, while co-transformation of 35S::*CUC2m::eGFP* and 35S::*gh-pre164* served as negative controls. The fluorescence intensity of 35S::*CUC2::eGFP* gradually decreased commensurately with increasing *gh-pre164* concentration (OD600 nm = 0.0–0.9) in the cells of tobacco leaves co-transformed with *gh-pre164* and 35S::*CUC2::eGFP* (Figure 2c,d). However, no change in fluorescence intensity was observed in

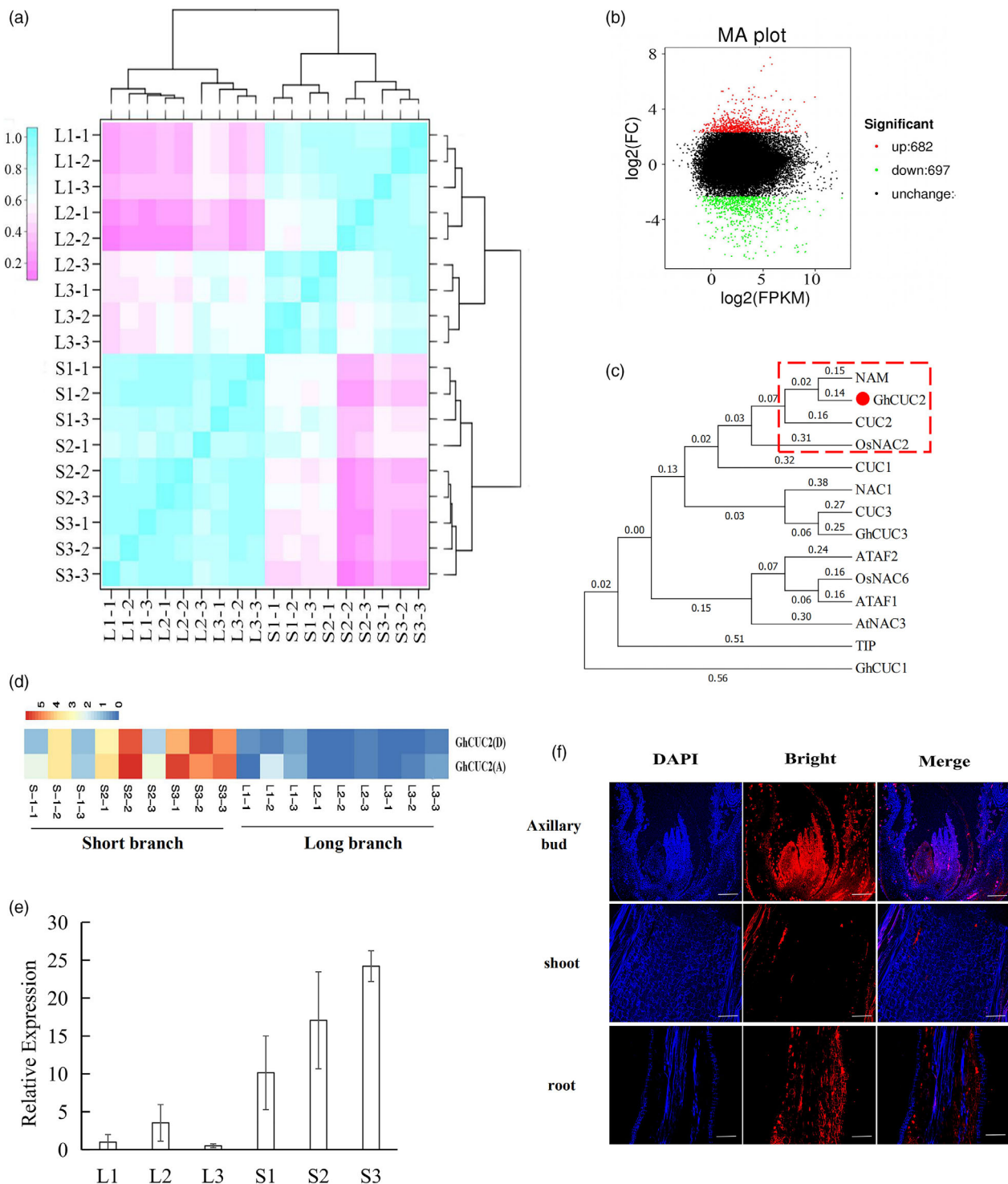


Figure 1 RNA-seq and cluster analysis show differential *GhCUC2* up-regulation in short-branch cotton. (a) Relative expression correlation analysis and cluster analysis between short- and long-branch cotton cultivars. (b) MA plot of differentially expressed genes (DEGs) for long-branch and short-branch cotton plants. (c) Unrooted phylogenetic tree of NAC transcription factors. Numbers between branches indicate bootstrap values based on 1000 replications. The red box indicates the CUC2 clade. Names and references for other NACs: *Arabidopsis thaliana*—ATAF1, ATAF2 (Aida et al., 1997), AtNAC2 (He et al., 2005), AtNAC3 (Takada et al., 2001), AtNAM (Duval et al., 2002), CUC1, CUC2 (Takada et al., 2001), CUC3 (Vroemen et al., 2003), NAC1 (Xie et al., 2000), NAC2, NAP (Sabrowski and Meyerowitz, 1998), TIP (Ren et al., 2000); *Oryza sativa*—OsNAC6 (Kusano et al., 2005; Ohnishi et al., 2005), OsNAC2 (Mao et al., 2007); *Petunia*—NAM (Souer et al., 1996). (d) *GhCUC2* expression levels among long-branch and short-branch cotton plants based on RNA-seq. (e) qRT-PCR detection of relative expression of *GhCUC2* among long-branch and short-branch cotton plants. (f) Fluorescence *in situ* hybridization (FISH) detection of *GhCUC2* in different tissues. Blue, DAPI; Red, *GhCUC2*; Scale bars = 100 μ m.

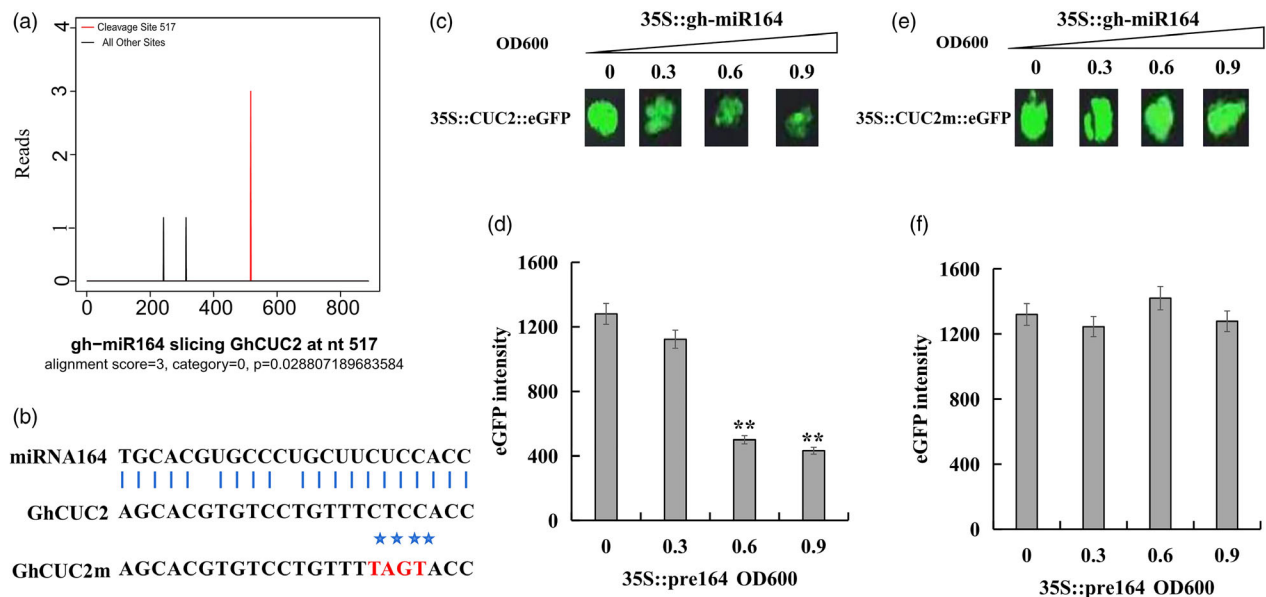


Figure 2 miR164 directly cleaves *GhCUC2* transcripts. (a) Cleavage positions predicted from degradome data. Red peak indicates the miR164 cleavage site position. (b) Sequence alignment of miR164, *GhCUC2* and *GhCUC2m*. Red letters indicate nonsynonymous substituted nucleotides in the miR164 target site that disrupt miR164-mediated cleavage without altering translated amino acid residues. Blue lines indicate Watson-Crick base pairing between the *GhCUC2* mRNA and miR164. Mismatches are indicated by stars. (c) Tobacco leaf cells transiently expressing eGFP::CUC2 (OD600 nm = 0.6) or (e) eGFP::CUC2m (OD600 nm = 0.6) alone or co-expressed with miR164 (OD600 nm = 0.3/0.6/0.9). eGFP::CUC2 protein accumulation decreases with increasing miR164 concentration. (d) and (f) Change in eGFP intensity with increasing miR164 concentration. Results represent the mean \pm SD of three independent experiments. Significance was determined by *t*-test; ** indicates $P < 0.01$.

the tobacco leaves co-transformed with *gh-pre164* and mutated 35s::CUC2m::eGFP (Figure 2e,f), regardless of increasing *gh-pre164* concentration (OD600 nm = 0.0–0.9). We also performed 5' RLM-RACE and found that the *GhCUC2* target site is cleaved at position 11 starting from the 5' end (Figure S2). Overall, these findings indicated that miR164 specifically cleaved CUC2 mRNA at the predicted target sequence and thereby suppressed the accumulation of CUC2 protein.

miR164-CUC2 module regulates branching in cotton and *Arabidopsis*

To assess the potential biological functions of miR164 and *GhCUC2* in regulation of plant architecture, we generated transgenic *Arabidopsis* lines overexpressing miR164 (OE-*gh-pre164*), *GhCUC2* (OE-*GhCUC2*) and *GhCUC2m* (OE-*GhCUC2m*) under the control of the *CaMV35S* promoter (Figure 3a). Their expression levels were confirmed using semi-quantitative PCR, which indicated successful overexpression in transgenic lines relative to wild type (WT; Figure 3d,e). The OE-*gh-pre164* plants exhibited a significantly higher branch number than WT, while the OE-*GhCUC2* and OE-*GhCUC2m* lines had significantly fewer branches than WT (Figure 3b). In addition, the majority of OE-*GhCUC2m* and OE-*GhCUC2* transgenic seedlings produced similar numbers of lateral branches, although these lateral branches were significantly shorter on average in the OE-*GhCUC2m* line ($P < 0.01$) compared with those of the OE-*GhCUC2* line (Figure 3c). These results indicated that CUC2m blocked the cleavage of miR164, which was supported by higher CUC2 transcript levels in the OE-*GhCUC2m* transgenic line compared with the OE-*GhCUC2* line (Figure 3d,e), thus suggesting that higher CUC2 expression resulted in shorter branches.

To further investigate the putative biological function of *GhCUC2* and miR164 in cotton, a CLCrV-based virus-induced gene silencing (VIGS) strategy was used to knock down the expression of *GhCUC2* (pCLCrV::*GhCUC2*) and miR164 (short tandem target mimic RNA of miR164, STTM164), and to overexpress miR164 (pCLCrV::*gh-pre164*) in cotton. Plants with high silencing efficiency were selected for greenhouse cultivation, and their phenotypes were observed at 70 days (Figure S3). Compared with WT, the STTM164 plants exhibited significantly shorter branches (Figure 4a), while the pCLCrV::*GhCUC2* and pCLCrV::*pre164* plants had no obvious, visible differences from vector control plants (Figure 4b,c). We thus proposed that increased CUC2 expression in STTM164 plants potentially resulted in decreased branch length, whereas decreased CUC2 expression levels in pCLCrV::*GhCUC2* and pCLCrV::*pre164* plants had no effect on branch development.

Considering that CUC2 can be cleaved by miR164, while CUC2m disrupted CUC2 suppression by miR164, we subsequently overexpressed *GhCUC2m* in wild-type cotton to investigate its possible function in branch development. To generate these plants, we cloned the full-length CUC2m gene fragment into the pCambia2300 plant overexpression vector, then transferred the vector construct into WT cotton, resulting in six independent transgenic lines. Overexpression transgenic lines OE1, OE2 and OE3 were selected for further observation of CUC2-related phenotypes among progeny. Overexpression levels in the T₁ generation of these lines were evaluated by semi-quantitative PCR (Figure S4). We found that the branch lengths among the OE plants were significantly shorter compared with WT (Figures 4d,e, f and S4). Taken together, our data strongly suggest that miR164 mediates the cleavage of CUC2 transcripts and that the CUC2 transcription factor regulates lateral branch development.

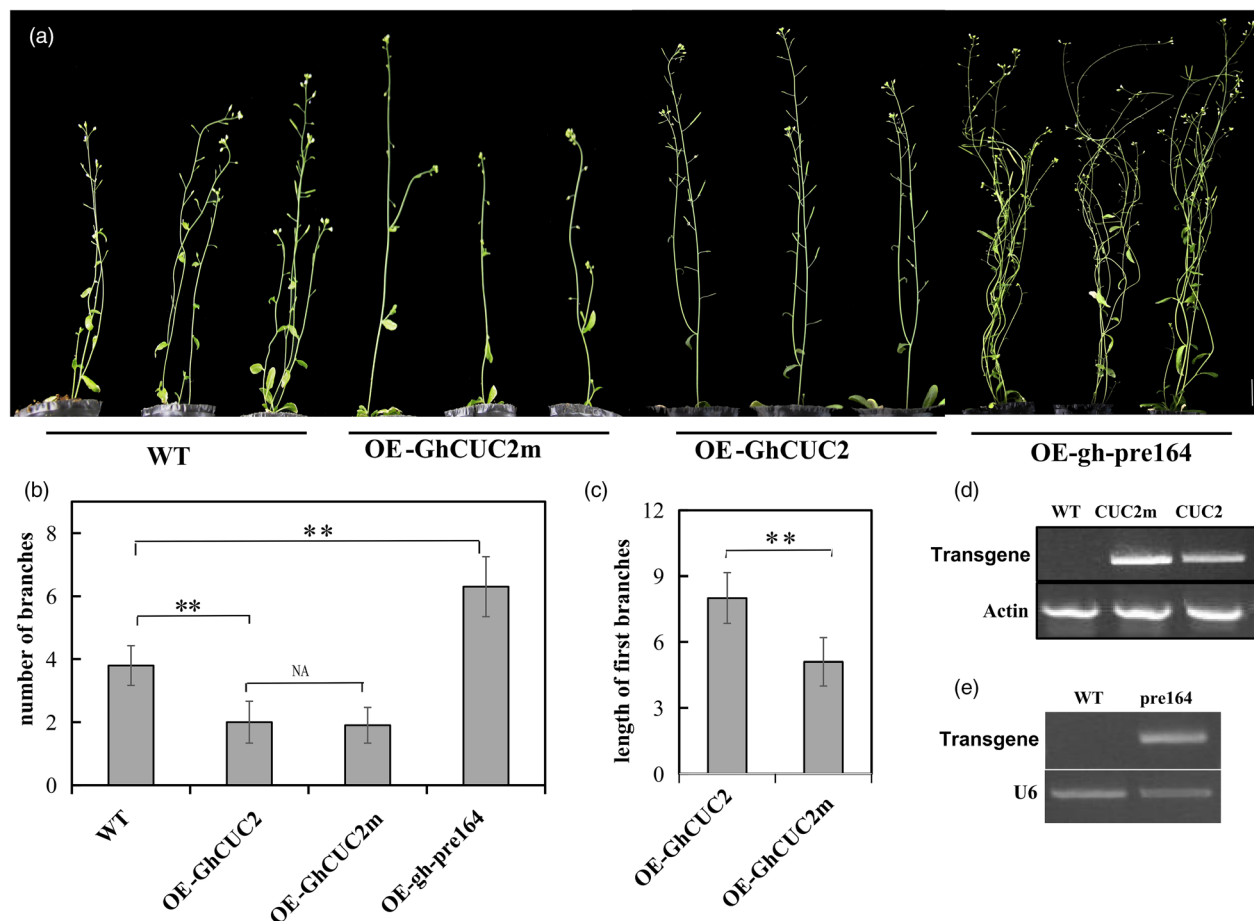


Figure 3 *GhCUC2* and miR164 regulate branch development in *Arabidopsis*. (a) Phenotypic analysis of *35S::GhCUC2*, *35S::GhCUC2m* and *35S::pre164* transgenic *Arabidopsis* overexpression lines at 30 days after emergence (DAE). Scale bar, 2 cm. (b) Statistical analysis of branch number in wild-type (WT), OE-GhCUC2, OE-GhCUC2m and OE-gh-pre164 *Arabidopsis* at 40 DAE. (c) Statistical analysis of branch length phenotype between OE-GhCUC2 and OE-GhCUC2m *Arabidopsis* overexpression lines. (d) Semi-quantitative PCR detection of *GhCUC2* mRNA levels in WT, OE-GhCUC2 and OE-GhCUC2m *Arabidopsis* lines. The *Actin* gene served as an internal reference. (e) Semi-quantitative PCR detection of miR164 transcripts in OE-gh-pre164 *Arabidopsis*. The *U6* gene served as an internal reference.

GhCUC2 interacts with GhBRC1 *in vitro* and *in vivo*

The BRC1 transcription factor has been shown to regulate plant development, including aspects of branch architecture (Alice *et al.*, 2020; Diao *et al.*, 2019). *AtBRC1* was shown to arrest axillary bud development and prevent axillary bud outgrowth, while *brc1* mutant plants produced more branches (Aguilar-Martínez *et al.*, 2007). To analyse *GhBRC1* function in branching development, we transformed plants from an *Arabidopsis brc1* mutant line with *GhBRC1* to observe whether it could rescue the high branch number phenotype. As expected, *GhBRC1* overexpression in the *brc1* mutant significantly decreased the rosette-leaf branch number by half, compared with that of the *brc1* mutant (Figure 5a,b). *GhBRC1* shares the conserved TCP domain with *AtBRC1*, thus supporting the conserved and essential role of *BRC1* in regulating bud formation and shoot architecture (Figure S5).

We then performed FISH assays to examine the expression patterns of *GhBRC1* in cotton and found that they were consistent with that of *GhCUC2* expression (Figures 1e and 5c). We speculated that the short-branch phenotype in *GhCUC2*-overexpressing cotton plants may be related to an interaction between *GhCUC2* and *GhBRC1*, and that they both participate in

a common pathway to regulate branch development. To test this hypothesis, we conducted a yeast two-hybrid (Y2H) assay, which revealed a strong interaction between *GhBRC1* and *GhCUC2* (Figure 5d). We next performed a bimolecular fluorescence complementation (BiFC) assay. *Agrobacterium tumefaciens* cells carrying the *GhBRC1*-YFPN and *GhCUC2*-YFPC plasmids were co-infiltrated into the lower epidermis of tobacco leaves. After a 72-h incubation, a strong YFP fluorescence signal was detected (Figure 5e). In contrast, YFP fluorescence was undetectable in the negative control samples, confirming that *GhBRC1* and *GhCUC2* interacted *in planta*. We then used pull-down and Co-IP assays to further validate the interactions of the *GhCUC2* proteins with *GhBRC1*. A direct physical interaction *in vitro* was also observed in GST pull-down assays (Figure 5g), and the Co-IP result also supported that *GhCUC2* interacted with *GhBRC1* *in planta* (Figure 5f).

GhCUC2 and *GhBRC1* negatively regulate branching via activating *NCED1* expression

TCP genes have been shown to regulate abscisic acid (ABA) signalling pathway genes. For example, *ABI3* and *ABI4* were up-regulated in *OsTCP19* overexpressing plants (Mukhopadhyay and

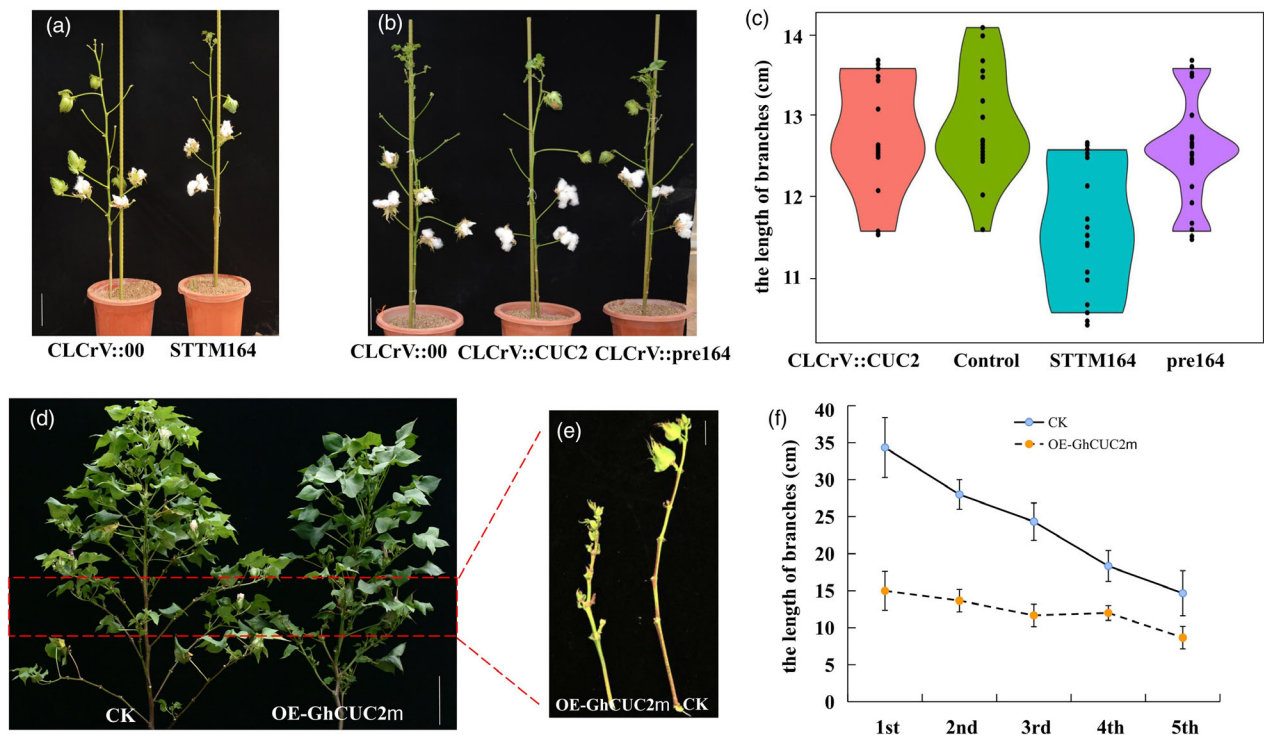


Figure 4 miR164 and *GhCUC2* regulate branch length in cotton. (a) Representative images showing morphological and growth phenotypes of STTM164 cotton plants silenced for miR164 (right) and empty vector controls (left). Scale bar, 10 cm. (b) Representative images showing phenotypes of empty vector control, CUC2-silenced cotton and miR164 overexpression cotton. (c) Distribution of branch lengths of CUC2-silenced, WT, miR164-silenced and miR164 overexpression cotton lines. (d) Phenotypic analysis of *GhCUC2m* transgenic cotton plants. Scale bar, 20 cm. (e) Image of branch phenotype in WT and OE-*GhCUC2m* cotton plants. Scale bar, 2 cm. (f) Statistical analysis of branch length in WT and OE-*GhCUC2m* cotton plants.

Tyagi, 2015). BRC1, itself a TCP family gene, together with the HB family genes, promotes the transcription of 9-CIS-EPOXICAROTENOID DIOXIGENASE3 (*NCED3*), a key enzyme in ABA biosynthesis, thereby leading to ABA accumulation and branching suppression (González-Grandío *et al.*, 2017). We examined our RNA-Seq data for expression of native *NCEDs* in OE-*GhCUC2m* cotton plants, and also validated these expression data in OE-*GhBRC1 Arabidopsis* plants using semi-quantitative PCR (Figure S6). The results showed that the expression of *NCED1* in both of these OE lines was increased, supporting that *NCED1* was indirectly or directly regulated by *CUC2* and *BRC1*.

To further elucidate whether *NCED1* served as a direct target of *GhBRC1* and *GhCUC2*, we used the Plant Regulation Data and Analysis Platform (http://plantregmap.cbi.pku.edu.cn/binding_site_prediction.php) to predict putative *NCED1*-binding sites in the ~2-kb promoter regions of these genes. This analysis revealed a GAGGAGACCACGT motif that could serve as a putative binding site in *GhBRC1*, while no binding motifs were detected in *GhCUC2*. To further determine whether the expression of *NCED1* is regulated by *GhBRC1*, the complete *NCED1* motif-enriched fragment pNCED1 and a mutated fragment lacking the binding site, pNCED1m, were each cloned into a pAbAi plasmid for yeast one-hybrid (Y1H) analysis. As indicated by the growth of yeast on the selective medium (–Leu/+AbA), *GhBRC1* could interact with pNCED1. By contrast, pNCED1m abolished binding by *GhBRC1*, indicating that *NCED1* transcription was directly regulated by *GhBRC1* (Figure 6a,b). In addition, an electrophoretic mobility shift assay (EMSA) using recombinant His-*GhBRC1* fusion protein showed that *GhBRC1*

was able to bind to a *NCED1* fragment (Figure 6c). Together, our results indicate that *GhBRC1* positively regulates ABA content through direct activation of *NCED1* expression.

Different from *GhBRC1*, transcriptional induction of *NCED1* may be indirectly modulated by *GhCUC2*. In order to validate whether *GhCUC2* and *GhBRC1* function together as a transcriptional activator complex of *NCED1* expression, we performed dual luciferase transactivation assays in *N. benthamiana* leaves. To this end, a ~2000 bp *NCED1* promoter fragment was cloned into the pGreenII0800-LUC vector to generate the reporter construct proNCED1-LUC. The coding sequences (CDSs) of *GhBRC1* and *GhCUC2* were individually fused into a pCambia2300 vector to generate the 35S-*GhBRC1* and 35S-*GhCUC2* effector plasmids (Figure S7). Then, with the pCambia2300 empty vector serving as a control, the 35S-*GhBRC1* and proNCED1-LUC constructs were co-infiltrated into *N. benthamiana* leaves. Analysis of LUC activity indicated that *GhBRC1* directly activated the promoter of *NCED1*. proNCED1-LUC and 35S-*GhCUC2* were also co-infiltrated with 35S-*GhBRC1*, resulting in extremely strong activation of the *NCED1* promoter (Figure 6d,e).

Consistent with the induction of *NCED1* expression, ABA content was significantly increased in axillary buds of STTM164 and OE-*GhCUC2m* cotton plants, compared with WT plants (Figure S8). These results cumulatively suggest that *GhCUC2* and *GhBRC1* together activated *NCED1* expression and ABA accumulation, and that this CUC2-mediated enhancement of *GhBRC1* regulatory activity could boost local ABA signalling and response in axillary buds (Figure 7).

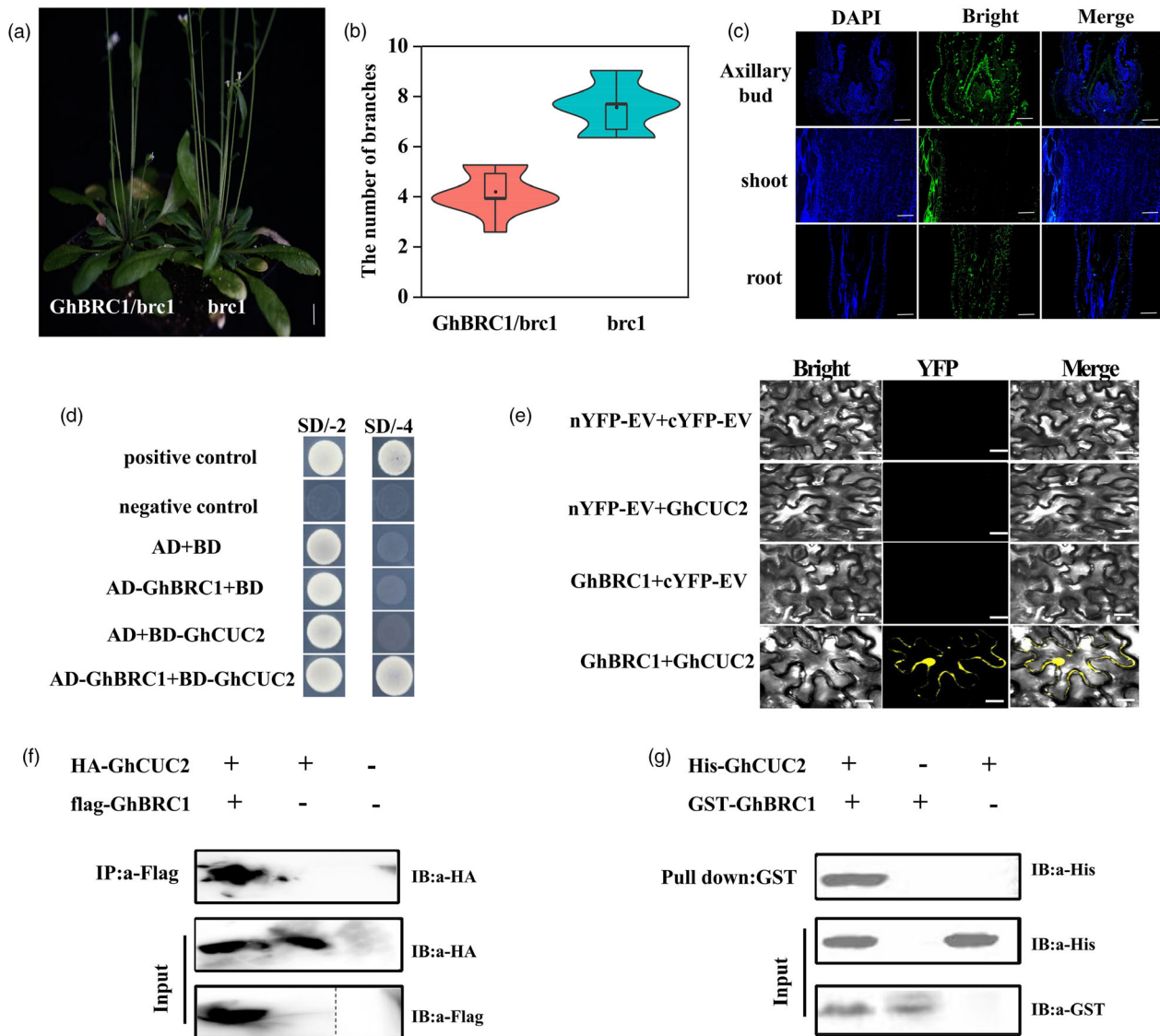


Figure 5 *GhCUC2* physically interacts with *GhBRC1* (a) Representative images of transgenic *brc1-2Arabidopsis* mutant (right) and *brc1-2* mutant carrying a 35S-*GhBRC1* complementation vector (left). (b) Quantitative analysis of rosette-leaf branches in 45-day-old *brc1-2* and transgenic plant. (c) Fluorescence *in situ* hybridization (FISH) detection of *GhBRC1* expression patterns in different tissues. Blue, DAPI; green, *GhBRC1*; Scale bars = 100 μ m. (d) Yeast two-hybrid (Y2H) detection of interaction between *GhCUC2* and *GhBRC1*. AD, pGADT7; BD, pGBDT7; SD, medium. (e) Bimolecular fluorescence complementation (BiFC) assay showing putative interaction between *GhBRC1* and *GhCUC2*. The N-terminus of yellow fluorescent protein (YFP) was fused to *GhBRC1*, while the C-terminus of YFP was fused to *GhCUC2*. EV, empty vector. Scale bars = 50 μ m. (f) *In vivo* co-immunoprecipitation (CoIP) assay. After the co-transformation of Flag-*GhBRC1* and HA-*GhCUC2* in *Nicotiana benthamiana* leaf, total proteins of *N. benthamiana* leaf were immunoprecipitated using an anti-HA antibody and were detected with anti-HA and anti-Flag antibodies. IB, immunoblot; IP, immunoprecipitation. (g) *In vitro* pull-down assay. Recombinant GST-*GhBRC1* and His-*GhCUC2* proteins were used for the pull-down assay. IB, immunoblot.

Discussion

Shoot branching in plants arises from axillary meristems in the region between the SAM and leaf primordia and is a major component driving plant architecture. The initiation of axillary meristems is a crucial step for generating axillary branches, and several genes have been identified for their effects on axillary meristem initiation. However, except for *SP*, *SFT* and *DREB1B* (Ji *et al.*, 2021; McGarry *et al.*, 2016; Si *et al.*, 2018), few genes controlling cotton branching architecture have been identified, and the molecular mechanism and genetic networks controlling this differentiation process during cotton branch

development remain unknown. Here, we uncovered a genetic and molecular framework in which a miR164-*GhCUC2*-*GhBRC1*-*GhNCED1* regulatory pathway controls the formation of axillary meristems, thereby determining plant architecture (Figure 7).

Phylogenetic analysis indicates that *GhCUC2* is grouped into the same subclade with *AtCUC2*, *OsNAC2* and petunia no apical meristem (NAM) proteins. These proteins are known to function in the development of the SAM and cotyledons, and to act in regulating lateral branch formation (Mao *et al.*, 2007; Souer *et al.*, 1996; Yu *et al.*, 2020). In *Arabidopsis thaliana*, the CUC2/CUC3-DA1-UBP15 regulatory module controls the initiation of

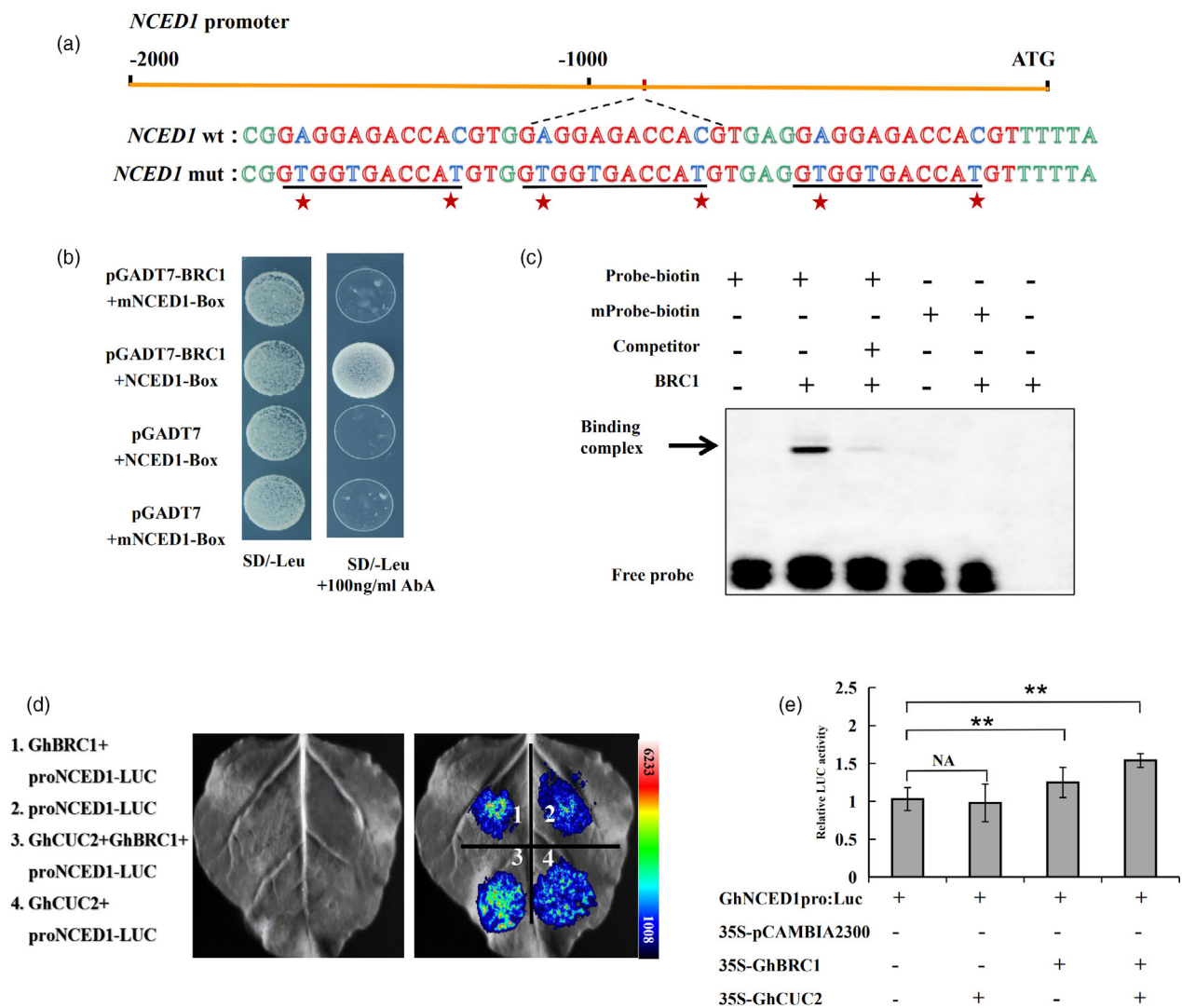


Figure 6 GhBRC1 binds to the promoter of *NCED1* and induces its transcription. (a) Alignment of the reporter constructs used in yeast one-hybrid (Y1H) analysis. Red stars indicate three tandem copies of the *NCED1* promoter core sequence in *NCED1* mutagenized promoter variant and WT, both of which were inserted into pAbAi as reporter constructs. (b) Y1H analysis showing that GhBRC1 binds the core sequence of *NCED1*, but not the *NCED1* mutated motif. SD/-Leu, SD medium without Leu; SD/-Leu/AbA¹⁰⁰, SD medium without Leu supplemented with 100 ng/mL AbA. (c) EMSA of GhBRC1 binding to the promoter of *GhNCED1* *in vitro*. A GhBRC1-His protein expressed in *Escherichia coli* was purified; its binding to biotin-labelled promoters was detected in the absence or presence of unlabelled wild-type probes (competitor). No specific binding was observed with the labelled mutant probes. (d) Luminescence imaging of dual-LUC assays showing interaction between GhCUC2 and GhBRC1 activates *GhNCED1* transcription in *Nicotiana benthamiana* leaf cells. PCambia2300 is empty vector; Gh BRC1+proNCED1-LUC is PCambia2300+Gh; BRC1+proNCED1-LUC proNCED1-LUC is 'PCambia2300+PCambia2300+proNCED1-LUC; and GhCUC2+GhBRC1+proNCED1-LUC is GhCUC2+GhBRC1+proNCED1-LUC GhCUC2+proNCED1-LUC is 'PCambia2300+GhCUC2+proNCED1-LUC. (e) Quantitative comparison of luciferase signals in (d). The error bars indicate mean \pm SD of three independent experiments. ***P* < 0.01, (Student's *t*-test).

axillary meristems, which determines the number of lateral branches (Yu *et al.*, 2020). The *NAM* gene of petunia is required for pattern formation in embryos and flowers, and embryos carrying the *nam* mutation fail to develop a SAM (Souer *et al.*, 1996). Overexpression of *OsNAC2* was found to increase tiller numbers in a dose-dependent way in rice, which is in agreement with the phenotype of the *Ostil1* mutant (Mao *et al.*, 2007). In this study, we found that *GhCUC2* was preferentially expressed in axillary buds to regulate bud outgrowth in cotton. *GhCUC2* transgenic overexpression lines showed reduced branch length, consistent with the phenotype exhibited by STTM164 plants. Furthermore, we observed that OE-GhCUC2 and OE-GhCUC2m

displayed fewer axillary branches, as opposed to OE-pre164 in *Arabidopsis*, indicating that miR164-CUC2 regulatory module function is conserved in the initiation of plant axillary meristems. ABA is well-established as a negative regulator of axillary bud growth in *Arabidopsis*, rice and soybean; studies examining a wide variety of species showed that ABA abundance in buds is negatively correlated with bud development (Luo *et al.*, 2019; Tamas *et al.*, 1979; Yao and Finlayson, 2015). In *Arabidopsis*, mutation of the ABA biosynthetic genes *NCED3* and *ABA2* enhanced branching and confirmed an inverse correlation between bud growth potential and bud ABA levels (Reddy *et al.*, 2013). ABA levels were reduced in the lower buds of

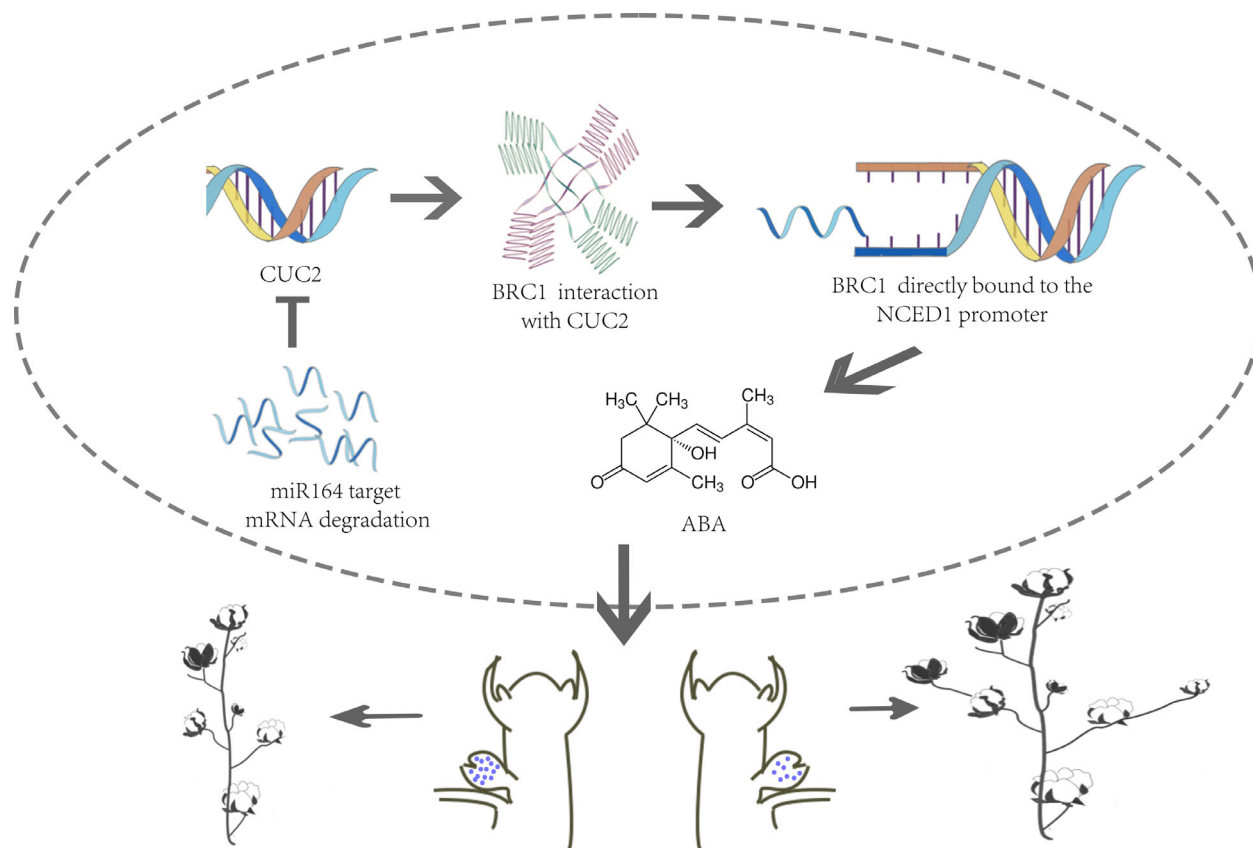


Figure 7 Proposed model of how miR164-GhCUC2-GhBRC1 module regulates plant architecture through ABA in cotton. The number of dots indicates the content of ABA.

hyperbranching mutants deficient for auxin signalling (AUXIN RESISTANT1) and BRANCHED1 (BRC1) function (Yao and Finlayson, 2015). *BRC1* expression was not affected by exogenous ABA in buds, strongly suggesting that ABA signalling functions downstream of *BRC1*. However, the expression of TAA1, an indole-3-acetic acid (IAA) biosynthetic enzyme, and the auxin transporter PIN1, were both suppressed by ABA in buds, suggesting that ABA may inhibit bud growth in part by controlling IAA biosynthesis and transport locally (Yao and Finlayson, 2015). In our study, we analysed transcript levels of *NCEDs*, as well as that of auxin biosynthesis and transport genes, using three independent *GhCUC2m* overexpression cotton lines. We found that *NCED1* was significantly up-regulated but *PIN4* was significantly decreased in OE lines compared with WT, indicating that *CUC2* regulates branch development via increasing the accumulation of ABA and inhibiting auxin transport. Moreover, manipulating miR164 levels or expressing cleavage-resistant *CUC2m* transcripts clearly demonstrated that miR164 functions as a negative regulator of ABA-mediated lateral branch development by controlling *CUC2* mRNA levels.

In recent years, the network consisting of *BRC1* and its downstream targets has been characterized. *BRC1* has been called a branching integrator because it acts downstream of many other pathways that influence branching, including the strigolactone pathway (Braun *et al.*, 2011), auxin (Aguilar-Martínez *et al.*, 2007), ABA (González-Grandío *et al.*, 2017), cytokinins (Stes *et al.*, 2015), decapitation (Gao *et al.*, 2016) and R:FR response (González-Grandío *et al.*, 2013). A previous study showed that ABA affects branching independently of

BRC1, and that *BRC1* promoted the accumulation of ABA in lower buds. Therefore, ABA more likely acts downstream of *BRC1* to transduce the effects of *BRC1* function (Yao and Finlayson, 2015). In our study, genetic analyses and biochemistry assays suggested that *GhBRC1* functions, at least in part, in a common pathway with *CUC2* to regulate axillary meristem initiation. We found that *GhBRC1* directly associates with the *NCED1* promoter region to induce its transcriptional expression, and consequently, ABA accumulation. Protein interactions between *CUC2* and *GhBRC1*, as well as the similar phenotypes resulting from *CUC2* and *BRC1* overexpression in cotton and *Arabidopsis*, together support that *GhBRC1* functions synergistically with *GhCUC2* in regulating axillary meristem initiation. Furthermore, our study shows that *BRC1* directly triggers an *NCED1*-mediated cascade, which ultimately boosts local ABA accumulation. Here, we provide evidence that *CUC2*-*BRC1*-*NCED1* function in a common pathway to control the initiation of axillary meristems.

Taken together, our findings point to a genetic and molecular framework in which a miR164-*CUC2*-*BRC1*-*NCED1* regulatory module mediates axillary meristem initiation to control lateral branch architecture in plants. This pathway enriched the regulatory network controlling cotton architecture and provided candidate genes for precisely modulating cotton architecture. This plant short-branch trait greatly improves cotton yield by allowing high planting density. Extensive planting globally of varieties with short branches would increase cotton fibre yield. Therefore, a short-branching trait represents an ideal plant type for cotton breeding.

Experimental procedures

Plants materials

All *Arabidopsis thaliana* lines used here were derived from the Columbia-0 genetic background (Col). *Arabidopsis* and *Nicotiana benthamiana* were grown in a controlled environment at 22°C with a relative humidity of 60% under long-day conditions (16 h light/8 h dark) with white light illumination. Transgenic cotton plants were grown under natural field conditions in Anyang, China. The phytotron, with 28/20°C day/night temperature, 55%–70% relative humidity and a 14/10 h light/dark cycle, was used to culture cotton seedlings before they were transplanted to fields.

RNA isolation and real-time PCR analysis

First-strand cDNA was synthesized from total RNA using the FastQuant RT Kit (Tiangen Biotech). qRT-PCR was performed using SuperReal PreMix Plus Kit (SYBR Green; Tiangen Biotech). Gene-specific primers were listed in Table S2. UBQ was used as an endogenous reference gene.

For miRNA quantification, total RNA was extracted as described above, a poly (A) tail was added to the 3' end of RNA, and reverse transcription was initiated using the miRcute miRNA First-Strand cDNA Synthesis Kit (Tiangen). qRT-PCR was performed using an ABI StepOne Plus instrument (Applied Biosystems, Inc., Carlsbad, CA), and the $2^{-\Delta\Delta CT}$ method was used to calculate the relative expression level. U6 was used as an endogenous reference gene.

RNA-sequencing (RNA-seq) analysis

Three short-branch cultivars (Shan 4080, Jin7, Changrongzhongmian) and three long-branch cultivars (Zhong24, Zhong6, TM-1) were used as materials in this study. Total RNA was extracted, and RNA libraries were prepared by Beijing Genomics institution (BGI, Shenzhen, China). Three biological repeats were performed for the RNA-Seq experiment. The library products were sequenced using the Illumina HiSeq 2500 platform, generating paired-end reads. The raw data of RNA-seq were used to map reads to the reference genome TM-1 (AD1) genome NAU-NBI (Nanjing Agricultural University-Novogene Bioinformatics Technology) assembly v1.1 and annotated v1.1 (<https://www.cottongen.org>; Zhang *et al.*, 2015), NCBI, PANTHER, GO, KEGG or domain search against Pfam. Differentially expressed genes (DEGs) were defined as those having at least twofold change in expression (false discovery rate, FDR < 0.05).

Degradome sequencing

Total RNA was extracted from cotton leaf (Zhong24) using Trizol reagent (Invitrogen, Carlsbad, CA). Approximately, 200 µg total RNA was used to construct the degradome library. In brief, a 5' RNA oligonucleotide adaptor ligated to the fragments containing 5'-monophosphates using T4 RNA ligase. The first-strand cDNA was synthesized by reverse transcription using the ligated products with SuperScript™ II Reverse Transcriptase (Invitrogen) and then PCR-amplified. Next, the PCR products were digested with Mme I, and the 20-bp 'signatures' were captured to ligate a 3' adapter via T4 DNA ligase. The ligated products were finally amplified and used for degradome sequencing on an Illumina HiSeq 2000 at the Beijing Genomics Institute (BGI), Shenzhen, China.

Prediction of miRNA164 targets and miRNA target cleavage sites

To validate the miRNA/target interactions predicted based on degradome sequencing, we experimentally analysed their transient

co-expression in *N. benthamiana* leaves. We amplified CUC2 sequence from cDNA of cotton using a primer pair containing BamHI and SacI restriction sites as overhangs, and then, the amplified fragment was gel-purified and ligated into the pCambia2300(::GFP) vector. The mutated CUC2 variant CUC2m was produced by creating four mismatches in the miR164-binding sites without altering the amino acid sequences. The CUC2m sequence was also cloned in vector using the same method as for constructing the CUC2 vector. These vectors were delivered into *A. tumefaciens* GV3101 by the freeze-thaw method. We first pelleted and then gently resuspended the cells to the required final OD600 value and mixed the *Agrobacterium* suspension containing 35S::miR164 plasmid and 35S::CUC2 plasmid at a ratio of 1 : 1, then incubated for 1 h at room temperature. A syringe needle was used to force entry of the *Agrobacterium* suspension into the leaf. The plants were maintained at 20°C and shielded from direct light by placing them under a table surrounded with black plastic for 24 h. Plants were grown on soil in a 16 h light/8 h dark cycle at 20 °C, and the leaves were collected at approximately 72 h post infiltration for GFP fluorescence detection and RT-PCR.

RLM-RACE

To determine the miR164 cleavage site in CUC2, a RLM-RACE assay was performed with the RLM-RACE kit (Takara) according to the manufacturer's instruction. Total RNA was extracted from tobacco leaves. Approximately, 2 µg RNA was ligated to the RNA Oligo adaptor, the ligated RNA was used to synthesize cDNA using M-MLV reverse transcriptase according to the manufacturer's instructions. Two rounds of nested PCR were performed, after which the PCR products were inserted into a cloning vector for sequencing. The primers used in this assay are listed in Table S2.

Vector construction and plant transformation

We constructed all vectors using a one-step cloning method. This method uses a primer with a homologous arm and a double restriction site to amplify the gene fragment, which is then ligated to the vector with the same homologous arm and restriction site. All vectors were converted to *A. tumefaciens* strain GV3101/LB4404 using the freeze-thaw method.

pCambia2300 vector was used in this work to generate the overexpressing transgenic lines. gh-pre164 sequence was amplified from cotton genomic DNA, and CUC2 sequence was amplified from cDNA of cotton using primer pairs (Table S1), CUC2m sequence was synthesized, and then ligated into the vector pCambia2300 and confirmed by sequencing. *A. tumefaciens* containing gh-pre164, GhCUC2m and GhCUC2 plasmids were separately transformed into wild-type *Arabidopsis* (Col) by the floral dip method. Transgenic plants were selected with 50 µg/mL kanamycin on half-strength MS plates. OE-gh-pre164, OE-GhCUC2 and OE-GhCUC2m T2 single-copy lines were selected for the population study of lateral branching phenotype.

For cotton transformation, the detailed process was described in our previously published paper (Ge *et al.*, 2015). Transformants with different expression levels were selected for further analysis.

VIGS

Virus-induced gene silencing was performed as described previously (Gao *et al.*, 2011). A vector constructed with an miRNA precursor could result in high expression of the mature miRNA and a vector with an artificial small tandem target mimic (STTM) could lead to low expression of the mature miRNA. To create the miR164 overexpression vector pCLCrV-miR164, the precursor of

miR164 was amplified from total genomic DNA by PCR, verified by sequencing, and then introduced into the vector using the One-Step Cloning kit. For the miR164 suppression vector pCLCrV-STTM164, the STTM sequence of miR164 was designed and synthesized based Yan *et al.* (2012) and then introduced into the vector using the same kit. A diagram of STTM164 vector is shown in Figure S9, and the primers are listed in Table S1. The vector was introduced into *A. tumefaciens* GV3101. The *Agrobacterium* cultures were pelleted and resuspended. After 3 h incubation at room temperature, *Agrobacterium* harbouring pCLCrVA was mixed with an equal volume of *Agrobacterium* harbouring pCLCrVB. The mixed *Agrobacterium* solutions were infiltrated into the abaxial side of cotyledons of 7-day-old CR124 cotton seedlings using needleless syringes through small wounds, which were made on the surface of cotyledons or true leaves using small syringe needles. After the true leaves of the plants inoculated with CLCrV::CHL-expressing *Agrobacterium* showed a yellow phenotype, the young leaves from CLCrV::00, CLCrV::GhCUC2, STTM164, and CLCrV::pre164 plants were sampled for real-time PCR to check the interference efficiency and the expression levels of *GhCUC2* and miR164 (Figure S3).

BiFC assays

The BiFC assays for protein interaction detection were performed in *N. benthamiana* leaves using *A. tumefaciens*-mediated transient expression. Candidate interacting proteins were separately fused with the N- or C-terminal parts of the yellow fluorescent protein and then infiltrated into 3-week-old *N. benthamiana* leaves using syringes. At 48 h post infiltration, tissues were imaged with an LSM780 confocal laser-scanning microscope. Six independent *N. benthamiana* leaves were observed for analyses, and three biological replications were performed.

GST pull-down and co-immunoprecipitation

GhCUC2 without signal peptides were cloned into pGEX-4T-3 vectors as baits. GhBRC1 without signal peptides were cloned into pET32a vectors as preys. All the constructs were transformed into the *Escherichia coli* BL21 (DE3) strain to produce recombinant proteins. The pGEX-4T-3 vector was used to express glutathione-S-transferase (GST) as a negative control. Bait and prey proteins were mixed at 4 °C for 6 h and then purified using glutathione conjugated agarose beads (17-5132-01; GE Healthcare, San Ramon, CA). Next, the proteins were separated by 12% SDS-PAGE and immunoblotted with anti-GST or anti-His antibody (Proteintech, Rosemont, IL).

To validate the protein interactions of GhCUC2 and GhBRC1, co-immunoprecipitation (Co-IP) assays were performed as follows. 35S:Flag-GhCUC2 and 35S:HA-GhBRC1 were co-expressed in tobacco (*N. benthamiana*) leaves. Total proteins were isolated by homogenizing tissues with RIPA buffer 3 days after agroinfiltration. After centrifugation, the supernatant was incubated with 30 µL of HA-Myc-agarose conjugated beads (Sigma) for 3 h at 4 °C. The matrix beads were washed six times with immunoprecipitation buffer. All of the washing steps were carried out at 4 °C for 10 min and were followed by centrifugation at 1600×g. For immunoblot analysis, IP products and the input samples were separated by 12% sodium dodecyl sulphate-polyacrylamide gel electrophoresis (SDS-PAGE), and the target protein was detected by Western blot using anti-FLAG (1 : 1000, Sigma-Aldrich F1084) or anti-HA (1 : 1000, Abcam ab32) antibodies.

Yeast experiments

Y2H assays were performed using the GAL4-based two-hybrid system. The coding sequences (CDS) of *GhCUC2* were subcloned in-frame into pGADT7-Rec to generate pGAD-Preys. The coding regions of *GhBRC1* were cloned in-frame into pGBKT7 to generate pGBD-Baits. The corresponding primers are listed in Table S2. Then, pGBD-Baits and pGAD-Preys constructs were transformed into Y2HGold. Transformed cells were grown on synthetically defined (SD) medium lacking Leu or Trp for 4d. Then, the yeast cells were screened on synthetic dextrose selection medium lacking Leu, Trp, Hde and His (SD/-4).

In yeast one-hybrid (Y1H) experiments, the CDS of *GhBRC1* was cloned into the pGADT7 vector. The putative GhBRC1 binding motif in the NCED1 promoter sequence was selected and ligated into the pAbAi vector. The combination of pGADT7-GhBRC1 and the pAbAi-motif was transformed together into Y1HGold. Additionally, combinations of the empty vector pGADT7 and putative GhBRC1 binding motif, or mutated motif were also co-transformed into Y1HGold as negative controls. SD/Trp/Ura plates with appropriate nutrients were used to select the transformants, and positive clones were transferred to and grown on SD/Trp/Ura plates.

Dual-luciferase assay in *Nicotiana benthamiana*

The 2-kb GhNCED1 promoter sequence was cloned into the plant binary vector pGWB435, which was used as a reporter. The coding sequences of GhCUC2 and GhBRC1 were cloned into pCambia2300 vector, which was used as an effector. After sequencing, the verified plasmids were transformed into GV3101. The *Agrobacterium* harbouring reporter and effector constructs were co-infiltrated into *N. benthamiana* leaves. The empty pCambia2300 and pGWB435 vectors, the pCambia2300 vector with the reporter, and the effector with the pGWB435 empty vector were used as negative controls. Luciferase signals were captured and analysed using a Tanon 5200 Multi Chemiluminescent Imaging System (Tanon, Shanghai, China). Firefly luciferase (LUC) and *Renilla* luciferase (REN) activity levels were measured using a dual-luciferase reporter assay system (Promega). The measured LUC activity was normalized to that of REN.

Electrophoretic mobility shift assay (EMSA)

Electrophoretic mobility shift assays were carried out as described previously (Smith and Delbarygossart, 2001). The amplified CDS regions of GhBRC1 (Table S2) were fused in-frame with His tags and transformed into *E. coli* BL21. Oligonucleotide probes were synthesized and labelled with biotin at their 5' ends (Invitrogen). EMSAs were performed using the LightShift Chemiluminescent EMSA Kit (Thermo Fisher Scientific, Waltham, MA). The probes used in EMSA are listed in Table S2.

Fluorescence *in situ* hybridization

The partial-length cDNA fragments with fluorescent labels were synthesized by Sangon Biotech. The probe sequences for FISH are listed in Table S2. Western Blue plus 1 mM tetramisole was the substrate solution to reduce the hybridization background. Sample preparation and FISH experiments were carried out as described previously with slight modifications (Jackson *et al.*, 1994; Zhang *et al.*, 2013).

Extraction and quantification of endogenous hormone

About 0.1 g samples were harvested from axillary buds of WT, STTM164 and OE-GhCUC2 transgenic plants and used for measurement of hormone content. The extraction and quantification of endogenous hormones were performed using ELISAs by Shanghai Zhucai Biotechnology Co., Ltd. Three biological repeats were performed for each sample. Hormones were extracted by adding 500 μ L cold (v/v) aqueous methanol to each sample, and samples were mixed on an overhead shaker in the dark overnight. The extraction was repeated with 1 mL cold 80% MeOH. After the second extraction, samples were pre-purified with 500 μ L 80% aqueous methanol. Supernatants of the four extractions were pooled (Thermo Fisher Scientific). Tris-risermio Fisher Scientific) was then added up to 1 mL and samples were 1 : 10 diluted in 1x TBS for analysis.

Statistical analysis

All data were analysed using SigmaPlot 10.0 (Systat Software) and GraphPad Prism 5 (GraphPad Software) software. The averages and SD of all results were calculated, and ANOVA and Student's *t*-test were performed to generate *P* values. When there were statistically significant differences, Student-Newman-Kuels tests were conducted.

Acknowledgements

This research was financially supported by the National Natural Science Foundation of China (31621005, 31701476).

Conflict of interest

The authors declare no conflicts of interest.

Author contributions

LG, GY and ZJ designed the research; ZJ, CY, DY, WY, ZY, LS, WX and MY performed the research; GY, ZJ and CY analysed the data; LG, GY and ZJ wrote the paper.

References

- Aguilar-Martínez, J.A., Poza-Carrión, C. and Cubas, P. (2007) Arabidopsis BRANCHED1 acts as an integrator of branching signals within axillary buds. *Plant Cell*, **19**, 458–472.
- Aida, M., Ishida, T., Fukaki, H., Fujisawa, H. and Tasaka, M. (1997) Genes involved in organ separation in Arabidopsis: an analysis of the cup-shaped cotyledon mutant. *Plant Cell*, **9**, 841–857.
- Aida, M. and Tasaka, M. (2006) Genetic control of shoot organ boundaries. *Curr. Opin. Plant Biol.* **9**, 72–77.
- Alice, V., Priyanka, M., Adrian, R., Ulla, N., Karin, L. and Maria, C. (2020) Vernalization shapes shoot architecture and ensures the maintenance of dormant buds in the perennial *Arabis alpina*. *New Phytol.* **227**, 99–115.
- Braun, N., de Saint, G.A., Pillot, J.P., Boutet-Mercey, S., Dalmais, M., Antoniadi, I., Li, X. et al. (2011) The pea TCP transcription factor PsBRC1 acts downstream of Strigolactones to control shoot branching. *Plant Physiol.* **158**, 225–238.
- Chang, Z., Xu, R., Xun, Q., Liu, J., Zhong, T., Ding, Y. and Ding, C. (2020) OsmiR164-targeted OsNAM, a boundary gene, plays important roles in rice leaf and panicle development. *Plant J.* **106**, 41–55.
- Cui, X., Lu, F., Qiu, Q., Zhou, B., Gu, L., Zhang, S., Kang, Y. et al. (2016) REF6 recognizes a specific DNA sequence to demethylate H3K27me3 and regulate organ boundary formation in Arabidopsis. *Nat. Genet.* **48**, 694–699.
- Diao, Y., Zhan, J., Zhao, Y., Liu, L., Liu, P., Wei, X., Ding, Y. et al. (2019) GhTIE1 regulates branching through modulating the transcriptional activity of TCPs in cotton and Arabidopsis. *Front. Plant Sci.* **10**, 1348.
- Duval, M., Hsieh, F., Kim, Y. and Thomas, L. (2002) Molecular characterization of atnam: a member of thearabidopsis nac domain superfamily. *Plant Mol. Biol.* **50**, 237–248.
- Gao, X., Wheeler, T., Li, Z., Kenerley, C.M., He, P. and Shan, L. (2011) Silencing GhNDR1 and GhMKK2 compromises cotton resistance to Verticillium wilt. *Plant J.* **66**, 293–305.
- Gao, Y., Song, Z., Li, W., Jiao, F., Wang, R., Huang, C., Li, Y. et al. (2016) NtBRC1 suppresses axillary branching in tobacco after decapitation. *Genet. Mol. Res.* **15**(4). <https://pubmed.ncbi.nlm.nih.gov/25982315/>
- Ge, X., Zhang, C., Wang, Q., Yang, Z., Wang, Y., Zhang, X., Wu, Z. et al. (2015) iTRAQ protein profile differential analysis between somatic globular and cotyledonary embryos reveals stress, hormone, and respiration involved in increasing plantlet regeneration of *Gossypium hirsutum* L. *J. Proteome Res.* **14**, 268–278.
- González-Grandío, E., Pajaro, A., Franco-Zorrilla, J.M., Tarancón, C., Immink, R.G. and Cubas, P. (2017) Absciscic acid signaling is controlled by a BRANCHED1/HD-ZIPI cascade in Arabidopsis axillary buds. *Proc. Natl Acad. Sci. USA*, **114**, E245–E254.
- González-Grandío, E., Poza-Carrión, C., Sorzano, C.O. and Cubas, P. (2013) BRANCHED1 promotes axillary bud dormancy in response to shade in Arabidopsis. *Plant Cell*, **25**, 834–850.
- Greb, T., Clarenz, O., Schafer, E., Muller, D., Herrero, R., Schmitz, G. and Theres, K. (2003) Molecular analysis of the LATERAL SUPPRESSOR gene in Arabidopsis reveals a conserved control mechanism for axillary meristem formation. *Genes Dev.* **17**, 1175–1187.
- Guo, Y. and Gan, S. (2010) AtNAP, a NAC family transcription factor, has an important role in leaf senescence. *Plant J.* **46**, 601–612.
- He, X., Mu, R., Cao, W., Zhang, Z., Zhang, J. and Chen, S. (2005) AtNAC2, a transcription factor downstream of ethylene and auxin signaling pathways, is involved in salt stress response and lateral root development. *Plant J.* **44**, 903–916.
- Jackson, D., Veit, B. and Hake, S. (1994) Expression of maize KNOTTED1 relatedhomeobox genes in the shoot apical meristem predicts patterns of morphogenesis in the vegetative shoot. *Development*, **120**, 405–413.
- Ji, G., Liang, C., Cai, Y., Pan, Z., Meng, Z., Li, Y., Jia, Y. et al. (2021) A copy number variant at the HPDA-D12 locus confers compact plant architecture in cotton. *New Phytol.* **229**, 2091–2103.
- Kusano, H., Asano, T., Shimada, H. and Kadowaki, K. (2005) Molecular characterization of ONAC300, a novel NAC gene specifically expressed at early stages in various developing tissues of rice. *Mol. Genet. Genomics*, **272**, 616–626.
- Lee, M., Jeon, H., Kim, H. and Park, O. (2017) An Arabidopsis NAC transcription factor NAC4 promotes pathogen-induced cell death under negative regulation by microRNA164. *New Phytol.* **214**, 343–360.
- Li, X., Qian, Q., Fu, Z., Wang, Y., Xiong, G., Zeng, D., Wang, X. et al. (2003) Control of tillering in rice. *Nature*, **422**, 618–621.
- Li, Y., Xia, T., Gao, F. and Li, Y. (2020) Control of plant branching by the CUC2/CUC3-DA1-UBP15 regulatory module. *Plant Cell*, **32**, 1919–1932.
- Liu, M., Tan, X., Yang, Y., Liu, P., Zhang, X., Zhang, Y., Wang, L. et al. (2020) Analysis of the genetic architecture of maize kernel size traits by combined linkage and association mapping. *Plant Biotechnol. J.* **18**, 207–221.
- Luo, L., Takahashi, M., Kameoka, H., Qin, R., Shiga, T., Kanno, Y., Seo, M. et al. (2019) Developmental analysis of the early steps in strigolactone-mediated axillary bud dormancy in rice. *Plant J.* **97**, 1006–1021.
- Mao, C., Ding, W., Wu, Y., Yu, J., He, X., Shou, H. and Wu, P. (2007) Overexpression of a NAC-domain protein promotes shoot branching in rice. *New Phytol.* **176**, 288–298.
- Mathew, I.E. and Agarwal, P. (2018) May the fittest protein evolve: favoring the plant-specific origin and expansion of NAC transcription factors. *BioEssays*, **40**, e1800018.
- McGarry, R., Prewitt, S., Culpepper, S., Eshed, Y., Lifschitz, E. and Ayre, B. (2016) Monopodial and sympodial branching architecture in cotton is differentially regulated by the *Gossypium hirsutum* SINGLE FLOWER TRUSS and SELF-PRUNING orthologs. *New Phytol.* **212**, 244–258.

- Mitsuda, N., Seki, M., Shinozaki, K. and Ohme-Takagi, M. (2005) The NAC transcription factors NST1 and NST2 of Arabidopsis regulate secondary wall thickenings and are required for anther dehiscence. *Plant Cell*, **17**, 2993–3006.
- Mukhopadhyay, P. and Tyagi, A. (2015) OsTCP19 influences developmental and abiotic stress signaling by modulating ABI4-mediated pathways. *Sci. Rep.* **5**, 9998.
- Ohnishi, T., Sugahara, S., Yamada, T., Kikuchi, K., Yoshida, Y., Hirano, H. and Tsutsumi, N. (2005) OsNAC6, a member of the NAC gene family, is induced by various stresses in rice. *Genes Genet. Syst.* **80**, 135–139.
- Olsen, A.N., Ernst, H.A., Leggio, L.L. and Skriver, K. (2005) NAC transcription factors: structurally distinct, functionally diverse. *Trends Plant Sci.* **10**, 79–87.
- Poza-Carrión, C., Aguilar-Martínez, J.A. and Cubas, P. (2007) Role of TCP gene BRANCHED1 in the control of shoot branching in Arabidopsis. *Plant Signal Behav.* **2**, 551–552.
- Raman, S., Greb, T., Peaucelle, A., Blein, T., Laufs, P. and Theres, K. (2010) Interplay of miR164, CUP-SHAPED COTYLEDON genes and LATERAL SUPPRESSOR controls axillary meristem formation in *Arabidopsis thaliana*. *Plant J.* **55**, 65–76.
- Reddy, S., Holalu, S., Casal, J. and Finlayson, S. (2013) Abscisic acid regulates axillary bud outgrowth responses to the ratio of red to far-red light. *Plant Physiol.* **163**, 1047–1058.
- Ren, T., Qu, F. and Morris, T. (2000) HRT gene function requires interaction between a NAC protein and viral capsid protein to confer resistance to turnip crinkle virus. *Plant Cell*, **12**, 1917–1926.
- Saad, A., Li, X., Li, H., Huang, T., Gao, C., Guo, M., Cheng, W. *et al.* (2013) A rice stress-responsive NAC gene enhances tolerance of transgenic wheat to drought and salt stresses. *Plant Sci.* **203–204**, 33–40.
- Sablowski, R. and Meyerowitz, E. (1998) A homolog of NO APICAL MERISTEM is an immediate target of the floral homeotic genes APETALA3/PISTILLATA. *Cell*, **92**, 93–103.
- Schmitz, G., Tillmann, E., Carriero, F., Fiore, C., Cellini, F. and Theres, K. (2002) The tomato Blind gene encodes a MYB transcription factor that controls the formation of lateral meristems. *Proc. Natl Acad. Sci. USA*, **99**, 1064–1069.
- Schumacher, K., Schmitt, T., Rossberg, M., Schmitz, G. and Theres, K. (1999) The Lateral suppressor (Ls) gene of tomato encodes a new member of the VHLID protein family. *Proc. Natl Acad. Sci. USA*, **96**, 290–295.
- Si, Z., Liu, H., Zhu, J., Chen, J., Wang, Q., Fang, L., Gao, F. *et al.* (2018) Mutation of SELF-PRUNING homologs in cotton promotes short-branching plant architecture. *J. Exp. Bot.* **69**, 2543–2553.
- Smith, M. and Delbarygossart, S. (2001) Electrophoretic mobility shift assay (emsa). *Methods Mol. Med.* **50**, 249.
- Souer, E., van Houwelingen, A., Kloos, D., Mol, J. and Koes, R. (1996) The no apical meristem gene of Petunia is required for pattern formation in embryos and flowers and is expressed at meristem and primordia boundaries. *Cell*, **85**, 159–170.
- Stes, E., Depuydt, S., De Keyser, A., Matthys, C., Audenaert, K., Yoneyama, K., Werbrouck, S. *et al.* (2015) Strigolactones as an auxiliary hormonal defence mechanism against leafy gall syndrome in *Arabidopsis thaliana*. *J. Exp. Bot.* **66**, 5123–5134.
- Takada, S., Hibara, K., Ishida, T. and Tasaka, M. (2001) The CUP-SHAPED COTYLEDON1 gene of Arabidopsis regulates shoot apical meristem formation. *Development*, **128**, 1127–1135.
- Takeda, S., Hanano, K., Kariya, A., Shimizu, S., Zhao, L., Matsui, M., Tasaka, M. *et al.* (2011) CUP-SHAPED COTYLEDON1 transcription factor activates the expression of LSH4 and LSH3, two members of the ALOG gene family, in shoot organ boundary cells. *Plant J.* **66**, 1066–1077.
- Takeda, T., Suwa, Y., Suzuki, M., Kitano, H., Ueguchi-Tanaka, M., Ashikari, M., Matsuoka, M. *et al.* (2010) The OStB1 gene negatively regulates lateral branching in rice. *Plant J.* **33**, 513–520.
- Tamas, I., Ozbun, J. and Wallace, D. (1979) Effect of fruits on dormancy and abscisic acid concentration in the axillary buds of *Phaseolus vulgaris* L. *Plant Physiol.* **64**, 615–619.
- Vroemen, C., Mordhorst, A., Albrecht, C., Kwaaitaal, M. and de Vries, S. (2003) The CUP-SHAPED COTYLEDON3 gene is required for boundary and shoot meristem formation in Arabidopsis. *Plant Cell*, **15**, 1563–1577.
- Wang, B., Smith, S. and Li, J. (2018) Genetic regulation of shoot architecture. *Annu. Rev. Plant Biol.* **69**, 437–468.
- Wang, J., Bao, J., Zhou, B., Li, M., Li, X. and Jin, J. (2020) The osa-miR164 target OsCUC1 functions redundantly with OsCUC3 in controlling rice meristem/organ boundary specification. *New Phytol.* **229**, 1566–1581.
- Wang, Y. and Li, J. (2008) Molecular basis of plant architecture. *Annu. Rev. Plant Biol.* **59**, 253–279.
- Xie, Q., Frugis, G., Colgan, D. and Chua, N. (2000) Arabidopsis NAC1 transduces auxin signal downstream of TIR1 to promote lateral root development. *Genes Dev.* **14**, 3024–3036.
- Yan, J., Gu, Y., Jia, X., Kang, W., Pan, S., Tang, X., Chen, X. *et al.* (2012) Effective small RNA destruction by the expression of a short tandem target mimic in Arabidopsis. *Plant Cell*, **24**, 415–427.
- Yao, C. and Finlayson, S.A. (2015) Abscisic acid is a general negative regulator of arabidopsis axillary bud growth. *Plant Physiol.* **169**, 611–626.
- Yu, L., Tian, X., Fan, G. and Yunha, L. (2020) Control of plant branching by the CUC2/CUC3-DA1-UBP15 regulatory module. *Plant Cell*, **32**, 1919–1932.
- Yu, J., Ka, B. and Li, Z. (2014) Conserved miR164-targeted NAC genes negatively regulate drought resistance in rice. *J. Exp. Bot.* **65**, 2119–2135.
- Zhang, L., Guo, J., You, Q., Yi, X., Ling, Y., Xu, W., Hua, J., *et al.* (2015) GraP: platform for functional genomics analysis of Gossypium raimondii. *Database*, **2015**, bav047.
- Zhang, X., Zhou, Y., Ding, L., Wu, Z., Liu, R. and Meyerowitz, E.M. (2013) Transcription repressor HANABA TARANU controls flower development by integrating the actions of multiple hormones, floral organ specification genes, and GATA3 family genes in Arabidopsis. *Plant Cell*, **25**, 83–101.

Supporting information

Additional supporting information may be found online in the Supporting Information section at the end of the article.

Figure S1 (a) The sampling position on cotton plants for RNA-seq, Scale bars = 5 cm. (b) Statistical analysis of the 4th-branch length in short- and long-branch cotton cultivars.

Figure S2 The results of RLM-RACE.

Figure S3 Quantitative analysis of *GhCUC2* and *miR164* genes in CLCrV::00, STTM164, pre164 and pCLCrV-GhCUC2 cotton plants.

Figure S4 Expression levels of *GhCUC2* and phenotype images of *GhCUC2m* T₁ generation transgenic cotton plants, Scale bars = 10 cm.

Figure S5 Sequence alignment and domain analysis of *GhBRC1* in *Arabidopsis* and upland cotton.

Figure S6 (a) mRNA expression levels of *GhBRC1* and native *NCEDs* in *brc1* mutant and complemented OE-GhBRC1 *Arabidopsis* plants detected by semi-quantitative PCR. The *Actin* gene served as an internal reference. (b) Expression levels of *GhPIN4*, *GhNCED1*, and *GhCUC2* genes from RNA-seq data in the OE-GhCUC2m library.

Figure S7 Structural maps of the reporter, effector, and internal control plasmids used in the transient transactivation assay.

Figure S8 ABA, IAA, and GA contents in STTM164, OE-GhCUC2m, and WT cotton plants.

Figure S9 Structural map of STTM164 construct showing the design strategy for targeted suppression of GhmiR164 by artificial small tandem target mimic (STTM).

Table S1 DEGs between the two cultivar types (short-branch cultivar and long-branch cultivar)

Table S2 Primers used in this study
Supplementary Material